ICRC 2001

A search for 20÷100 TeV γ-rays from the Crab Nebula with 10 years of EAS-TOP data

P. L. Ghia, for the EAS-TOP Collaboration

Istituto di Cosmo-Geofisica del CNR, Torino, and INFN, Torino/LNGS, Italy

Abstract. The full dataset (1989-2000) of the EAS-TOP scintillator array has been exploited to search for γ-ray emission from the Crab Nebula at primary energies exceeding the typical ones of Cerenkov light detectors.

Different selection criteria have been applied to the data in order to select different primary energies, i.e., $E_1^{typ} = 20$ TeV and $E_2^{typ} = 100$ TeV.

The total ON-source time is 12925 hours, and the number of ON-source events are $N_1 = 1.2 \cdot 10^7$ and $N_2 = 1.3 \cdot 10^5$ (in angular windows $\Delta\Omega_1 \approx 2 \cdot 10^{-2}$ sr and $\Delta\Omega_2 \approx 3 \cdot 10^{-3}$ sr, respectively).

No D.C. emission has been detected: the 90% c.l. limits are $\Phi(> 20\text{TeV}) < 2.6 \cdot 10^{-13}\text{cm}^{-2}\text{s}^{-1}$, and $\Phi(> 100\text{TeV}) < 3.9 \cdot 10^{-14}\text{cm}^{-2}\text{s}^{-1}$. Using a power-law index of the Crab energy differential spectrum $\gamma = 2.5$ (as reported by Cerenkov light detectors), the obtained 90% c.l. differential flux limits are: $\frac{d\Phi}{dE} < 1.9 \cdot 10^{-14}\text{cm}^{-2}\text{s}^{-1}\text{TeV}^{-1}$, at 20 TeV, and $\frac{d\Phi}{dE} < 5.9 \cdot 10^{-16}\text{cm}^{-2}\text{s}^{-1}\text{TeV}^{-1}$, at 100 TeV.

1 Introduction

After the establishment of the Crab Nebula as a TeV γ-ray source by the Whipple group (Weekes et al., 1989), its VHE emission spectrum, up to $E_0 \approx 50$ TeV, has been extensively studied by atmospheric Cerenkov light detectors (Vacanti et al., 1991, Baillon et al., 1993, Goret et al., 1993, Konopelko et al., 1996, Hillas et al., 1998, Tanimori et al., 1994, 1998, Aharonian et al., 2000). In particular, at energy $E_0 \geq 10$ TeV, informations are provided through the large zenith angle technique (Hillas et al., 1998, Tanimori et al., 1998, Aharonian et al., 2000), while an additional measurement is reported by the high altitude air shower array, Tibet-ASγ (Amenomori et al., 1999).

Over the whole energy range, the spectrum is consistent with a power-law: VHE γ-rays are thought to be produced by

Correspondence to: P. L. Ghia
(Piera.Ghia@lngs.infn.it)

inverse Compton scattering between high energy electrons and ambient photons. However, at energies ≥ 10 TeV, the production mechanism for γ-rays due to nuclear p-p interactions and subsequent π^0 decays (Atoyan and Aharonian, 1996, Bednarek and Protheroe, 1997), could appear and become dominant. Thus, this energy region is of extreme interest, either to define the highest energy tail of the accelerated particles, or to identify the possible π^0-decay origin of γ-rays (therefore providing an observational evidence for the acceleration of cosmic rays in the Crab Nebula).

Here we report on the final analysis of ten years of data taken with the EAS-TOP scintillator array (Campo Imperatore, LNGS, 2005 m a.s.l.). The total ON-source time is 12925 hours, and the number of ON-source events are $N_1 = 1.2 \cdot 10^7$ and $N_2 = 1.3 \cdot 10^5$ (in angular windows $\Delta\Omega_1 \approx 2 \cdot 10^{-2}$ sr and $\Delta\Omega_2 \approx 3 \cdot 10^{-3}$ sr, respectively), at typical energy $E_1 = 20$ TeV and $E_2 = 100$ TeV, respectively.

We discuss the resolution, stability, and results of the observation.

2 The Experiment

The EAS-TOP Extensive Air Shower array, located at Campo Imperatore (2005 m a.s.l., lat. $42°27'$N, long. $13°34'$E, Gran Sasso Laboratories), has been in operation since January 1989 up to May 2000. A detailed description of the electromagnetic detector is given in Aglietta et al., 1993; here we summarize its main features.

In its final configuration, the array (progressively enlarged since 1989, see Table 1, where the different phases are summarized) consisted of 35 modules of scintillator counters, 10 m^2 each, distributed over an area $A \approx 10^5$ m^2. Except for eight modules, the array was organized in fifteen interconnected subarrays, each including a central module and five (or six) ones positioned on a circle of radius $r \approx 50 \div 80$ m. The trigger was provided by any fourfold coincidence of the central module and three adjacent modules of a subarray (threshold $n_p \approx 0.3$ m.i.p./mod.), the rate being $f \approx 35$

Table 1. The different configurations of the EAS-TOP array

Epoch	Scint. area [m²]	Enclosed area [m²]	Trigger condition	Trigger rate [Hz]
Feb.- Sep. 1989	240	8.10^4	7-fold	6
Oct. 1989 - Dec. 1990; Nov. 1991 - Oct. 1992	290	1.10^5	4-fold	30
Nov. 1992 - May 2000	350	$1.5 \cdot 10^5$	4-fold	35

Hz. Relative measurements of times of flight were performed within each subarray.

The full dataset (covering two operating intervals: January 1989 - December 1990, and November 1991 - May 2000) includes $\approx 8 \cdot 10^9$ showers.

3 Analysis

For γ-ray astronomy analysis (see Aglietta et al, 1995, for a detailed description), two subsets of data are constructed, in order to investigate different primary energies:

- high energy (HE) events: at least one full subarray fired (6-7 detectors), with the maximum number of particles detected by an inner module (i.e., core located inside the array boundary), rate $f_{HE} \approx 2$ Hz;

- low energy (LE) events: at least 4 adjacent detectors fired, without core location, rate $f_{LE} \approx 20$ Hz (≈ 5 Hz due to the minimum trigger configuration, i.e. 4 fired modules).

EAS arrival directions are determined for each event from the times of flight among the different modules. Events with reconstructed zenithal angle $\theta > 40°$ are not used in both sets.

3.1 Angular resolution

The reconstruction of the arrival directions are performed [1]

- for HE events, by using the timing information of the subarray located around the detector recording the largest number of particles; a plane approximation of the shower front is used, allowed by the fact that every module, being located in nearly symmetrical position around the core, is affected by nearly equal delays due to the EAS curvature and to sampling effects.

- for LE events, by averaging over every triggered subarray; a plane approximation is again allowed, due to the fact that the EAS core is not located, and the curvature effect cannot be taken into account (the effect will be included in the final angular resolution).

The angular resolution is determined:

- for HE events, by the measurement of the shape of the Moon shadow on the flux of primary cosmic rays (Aglietta et al., 1991, 1993), and by the odd-even subarray technique (Aglietta et al., 1993).

- for LE events, by the odd-even subarray technique only.
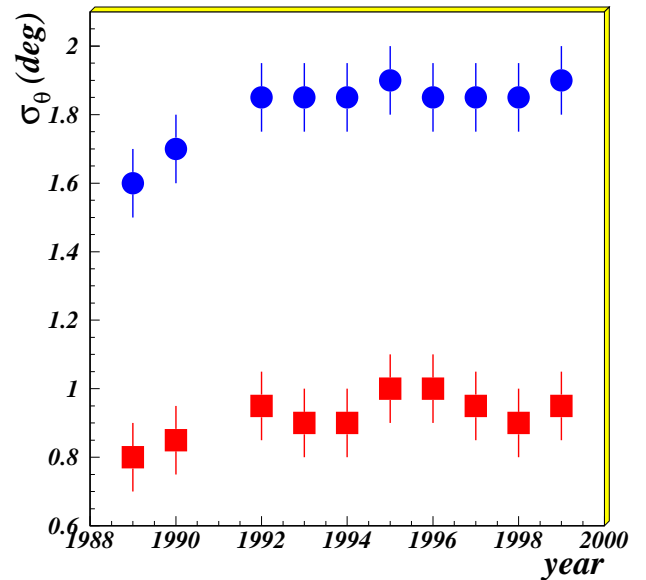
Fig. 1. Measured angular resolution vs year of operation: squares correspond to HE events, circles to LE ones.

The measured angular resolutions, which were monitored year by year (see Fig. 1 for the behavior versus year of operation) are:

- for HE events: $\sigma_\theta = 0.9 \pm 0.1°$, including systematic effects;

- for LE events [2] : $\sigma_\theta = 1.8 \pm 0.1°$, neglecting systematic errors. By adding the effect of EAS curvature (which is $0.03°$/m, versus core distance) at an average core distance $r \approx 60$ m (i.e. the mean radius of a subarray), we obtain $\sigma_\theta = 2.5°$.

---

[1] The relative timing of modules was calibrated every year (using a small reference scintillator counter), while, to compensate for variations in electronics or cables transit times, the time delays were renormalized on a 12 hours basis.

[2] If only four modules have triggered (rate ≈ 5 Hz), the angular resolution is worse: $\sigma_\theta = 4°$. Including systematic effects due both to the EAS curvature and to poor sampling, the angular resolution in this case can be evaluated to be $\sigma_\theta = 5.6°$.

	Entries	2350
	Mean	0.5036E-02
	RMS	0.9918

	Entries	2350
	Mean	-0.1074E-01
	RMS	0.9821
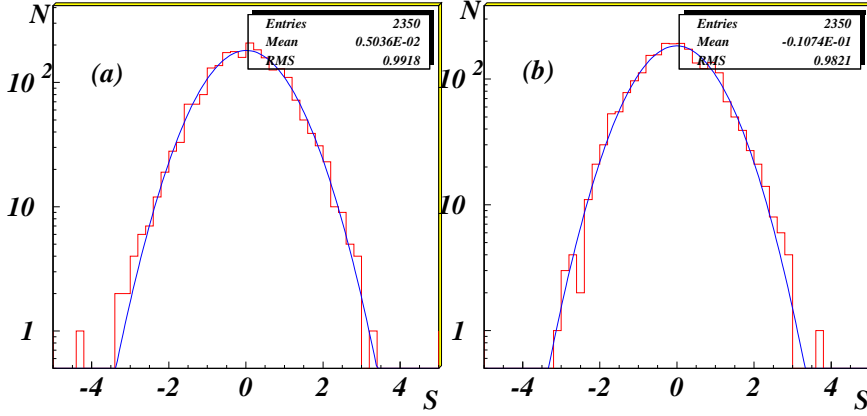
Fig. 2. Distributions of daily excesses from the Crab Nebula direction: (a) HE events, (b) LE events. The expected distributions based on Poissonian fluctuations are also shown, superimposed on the experimental ones.

3.2 Source search

The analysis is performed by searching for statistically significant excesses [3] in the number of counts inside a square bin of dimensions optimized on the angular resolution, centered on the source (ON), with respect to six analogous background bins (OFF). The dimensions of the bins (given in Table 2 together with the corresponding solid angles and angular efficiencies) are $\Delta\delta = 1.58\sigma_\theta$ and $\Delta\alpha = \Delta\delta/cos(\delta)$. The OFF bins are located at the same declination as the ON cell, and are shifted in right ascension of $\delta\alpha = \pm 2K\Delta\alpha$ (K=1,3).

The data are grouped in "source transits", defined as the passage of the source cell above the chosen horizon, corresponding to zenithal distance $\theta = 40°$, the exposure time, T_{exp}, being defined as the time between its rising and setting (for the Crab, $T_{exp} = 5.5$ h). We use only days in which all the seven cells, in both data subsets, are observed above the horizon without interruptions.

3.3 Background measurement and stability

The cosmic ray flux is the source of the counting rate background, and its measurement provides a test of the detector response to UHE atmospheric showers, and of its stability. This is done by comparing the measured EAS size spectrum (Aglietta et al., 1999) with the one expected from the extrapolation of the direct measurements at TeV energies. The agreement is quite good, thus proving that the behavior of the

---

[3] The significance, S (in units of standard deviations), of the number of observed events is computed according to the Li and Ma statistics (Li and Ma, 1983):

$$S = \sqrt{2}\left\{ N_{on}ln\left[\frac{1+\alpha}{\alpha}\left(\frac{N_{on}}{N_{on}+N_{off}}\right)\right] + \right.$$

$$\left. N_{off}ln\left[(1+\alpha)\left(\frac{N_{off}}{N_{on}+N_{off}}\right)\right]\right\}^{1/2}$$

where $\alpha = 1/6$.

Table 2. Characteristics of the different classes of events used for γ-ray astronomy.

Events class	HE	LE	LE (4 mod. only)
rate (Hz)	2	15	5
$\sigma_\theta(°)$	0.9	2.5	5.6
$\Delta\delta(°)$	1.5	4.0	4.0[a]
ang. eff. (ϵ)	0.9	0.8	0.3[b]
Ω (sr)	$2.7 \cdot 10^{-3}$	$1.9 \cdot 10^{-2}$	$1.9 \cdot 10^{-2}$

[a] To limit the time interval between ON and OFF observations, this is not optimized

[b] For LE events, weighting the angular efficiencies over the rate, we obtain that the total ϵ is 0.7.

detector is correct, and that the calculations of effective area and energy threshold (see sect. 3.4) are reliable.

The procedure of background measurement described in section 3.2 ensures that the ON and OFF bins are observed for the same exposure time at the same zenith angles. The closeness in time of such observations ($\pm$ 1 h) compensates for smooth variations of the experimental and atmospheric conditions during the source transit.

The fluctuations of the array counting rate have been studied through the distributions of the daily excesses, S, which are shown in Fig. 2 (a,b), for HE and LE subsets, respectively. They are relative to the whole period of measurement of the Crab (2350 days): comparing them with Gaussian distributions with mean value = 0 and s.d. = 1, we obtain a good agreement: for HE events $\chi^2 = 27.9$ for $\nu = 34$ degrees of freedom, for LE events $\chi^2 = 40.9$ for $\nu = 32$. The statistical behavior of the experimental fluctuations confirms the stability of the detector over such a long period of data taking.

3.4 Energy thresholds

The energy threshold E_0 is defined:

– for HE events, as the energy such that:

$$\int_0^\infty E^{-\gamma}A(E)dE = A_{eff}\int_{E_0}^\infty E^{-\gamma}dE$$

where A_{eff} is the saturation value for the array effective area, $A(E)$ [4], and γ is the assumed index of the differential source spectrum.

– for LE events, for which $A(E)$ is an increasing function of E, as the mode of the distribution $A(E)E^{-\gamma}$.

In both cases, the energy threshold depend on the assumed γ: its dependence on spectral index has been checked, resulting rather weak, i.e., $\Delta E_0/E_0 < 20\%$ for $\Delta\gamma = 0.7$.
Assuming a differential spectral index $\gamma = 2.5$ (see for example Aharonian et al., 2000), the energy thresholds for the Crab Nebula are: $E_{typ}^{HE} = 100$ TeV, and $E_{typ}^{LE} = 20$ TeV.

3.5 Flux and upper limit calculations

The number of photons with energy $E > E_0$ from a point source with energy spectrum $bE^{-\gamma}$ is:

$$n_\gamma = \epsilon T \int_0^\infty bE^{-\gamma} A(E) dE$$

where ϵ is the angular efficiency and T the exposure time.
The flux corresponding to n_{obs} observed events is:

$$\Phi(> E_\gamma) = \frac{1}{\int_0^\infty E^{-\gamma} A(E) dE} \frac{n_{obs}}{\epsilon T_{exp}(\gamma - 1)} E_\gamma^{-\gamma+1}$$

For HE events, for which the effective area A_{eff} is defined, this reduces to:

$$\Phi_\gamma(> E_0) = \frac{n_{obs}}{\epsilon T A_{eff}} \qquad (1)$$

The upper limits are then given by calculating n_{obs} at 90% c.l. following Helene, 1983.

4 Results

The total database includes 2350 transits of the Crab Nebula (corresponding to total ON-source time of 12925 h), the number of collected showers being:

– HE events: $N_{ON} = 133474$, $N_{<OFF>} = 133111.7$, $S = +0.9$

– LE events: $N_{ON} = 12350146$, $N_{<OFF>} = 12351708$, $S = -0.4$.

Using a power-law index for the differential energy spectrum of the Crab, $\gamma=2.5$, the 90% c.l. integral flux limits are:

– $\Phi(> 20\text{TeV}) < 2.6 \cdot 10^{-13}\text{cm}^{-2}\text{s}^{-1}$

– $\Phi(> 100\text{TeV}) < 3.9 \cdot 10^{-14}\text{cm}^{-2}\text{s}^{-1}$

Consequently, the 90% c.l. differential flux limits are:

– $\frac{d\Phi}{dE} < 1.9 \cdot 10^{-14}\text{cm}^{-2}\text{s}^{-1}\text{TeV}^{-1}$, at 20 TeV

– $\frac{d\Phi}{dE} < 5.9 \cdot 10^{-16}\text{cm}^{-2}\text{s}^{-1}\text{TeV}^{-1}$, at 100 TeV

These are shown in Fig. 3, together with existing measurements.

---

[4] $A(E)$ is the array effective area as a function of the primary energy E, calculated through a simulation including both the cascade development in the atmosphere and the detector response.
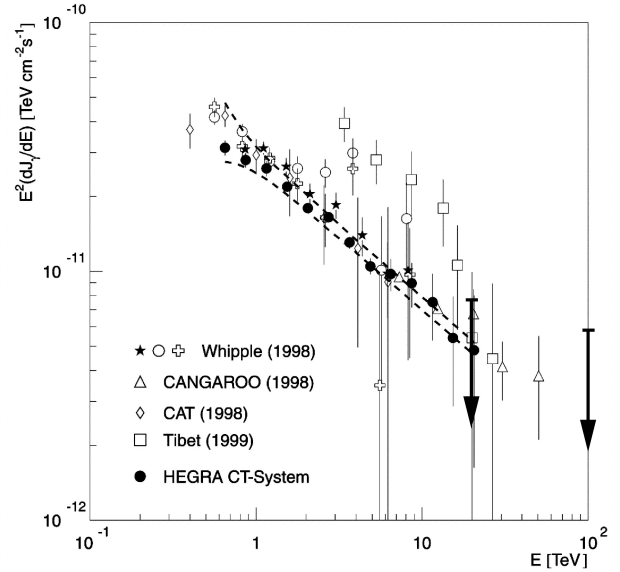
Fig. 3. Summary of VHE γ-ray data from the Crab Nebula (from Aharonian et al., 2000). Upper limits from the present work are indicated as large arrows.

References

Aglietta, M. et al., Proc. 22nd ICRC, Dublin, Ireland, 1991, vol.2, 708-711

Aglietta, M. et al., Nucl. Instr. and Meth., A336, 310–321, 1993

Aglietta, M. et al., A. Ph., 3, 1–15, 1995

Aglietta, M. et al., A. Ph., 10, 1–9, 1999

Aharonian F.A. et al., Ap. J., 539, 317–324, 2000

Amenomori, M., Ayabe, S., Cao, P. Y., et al., Ap. J., 525, L93–L96, 1999

Atoyan, A.M. and Aharonian, F.A., Mon. Not. R. Astron. Soc., 278, 525–541, 1996

Baillon, P., Behr, L., Danagoulian, S., et al., A. Ph., 1, 341–355, 1993

Bednarek, W. and Protheroe, R.J., Phys. Rev. Letts., 79, 2616–2619, 1997

Goret, P., Palfrey, T., Tabary, A., et al., A&A, 270, 401–406, 1993

Helene O., Nucl. Instr. Meth. 212, 319, 1983

Hillas A.M., et al., Ap. J., 503, 744–759, 1998

Konopelko, A., Aharonian, F., Akhperjanian, A., et al., A. Ph., 4, 199–215, 1996

Li, T.P. and Ma, Y.Q, Ap.J., 272, 317–324, 1983

Tanimori, T., Tsukagoshi, T., Kifune, T., et al., Ap. J., 429, L61–L64, 1994

Tanimori, T., Sakurazawa, K., Dazeley, S. A., et al., Ap. J., 492, L33–L36, 1998

Vacanti G., Cawley M.F., Colombo E., et al., Ap. J., 377, 467–479, 1991

Weekes T.C., Cawley M.F., Fegan D.J., et al., Ap. J., 342, 379–395, 1989